

The evolution of X-ray emission in young stars

Thomas Preibisch¹

and

Eric D. Feigelson²

ABSTRACT

The evolution of magnetic activity in late-type stars is part of the intertwined rotation-age-activity relation which provides an empirical foundation to the theory of magnetic dynamos. We study the age-activity relation in the pre-main sequence (PMS) regime, for the first time using mass-stratified subsamples. The effort is based on the *Chandra* Orion Ultradeep Project (COUP) which provides very sensitive and homogenous X-ray data on a uniquely large sample of 481 optically well-characterized low-extinction low-mass members of the Orion Nebula Cluster, for which individual stellar masses and ages could be determined. More than 98 percent of the stars in this sample are detected as X-ray sources.

Within the PMS phase for stellar ages in the range $\sim 0.1 - 10$ Myr, we establish a mild decay in activity with stellar age τ roughly as $L_X \propto \tau^{-1/3}$. On longer timescales, when the Orion stars are compared to main sequence stars, the X-ray luminosity decay law for stars in the $0.5 < M < 1.2 M_\odot$ mass range is more rapid with $L_X \propto \tau^{-0.75}$ over the wide range of ages $5 < \log \tau < 9.5$ yr. When the fractional X-ray luminosity L_X/L_{bol} and the X-ray surface flux are considered as activity indicators, the decay law index is similarly slow for the first 1 – 100 Myr but accelerates for older stars. The magnetic activity history for M stars with masses $0.1 < M < 0.4 M_\odot$ is distinctly different. Only a mild decrease in X-ray luminosity, and even a mild increase in L_X/L_{bol} and F_X , is seen over the 1 – 100 Myr range, though the X-ray emission does decay over long timescales on the main sequence.

Together with COUP results on the absence of a rotation-activity relation in Orion stars, we find that the activity-age decay is strong across the entire history

¹Max-Planck-Institut für Radioastronomie, Auf dem Hügel 69, D-53121 Bonn, Germany

²Department of Astronomy & Astrophysics, Pennsylvania State University, University Park PA 16802

of solar-type stars but is not attributable to rotational deceleration during the early epochs. A combination of tachocline and distributed convective dynamos may be operative in young solar-type stars. The results for the lowest mass stars are most easily understood by the dominance of convective dynamos during both the PMS and main sequence phases.

Subject headings: open clusters and associations: individual (Orion Nebula Cluster) - stars: activity - stars: pre-main sequence - stars: low-mass - X-rays: stars

1. Introduction

The magnetic activity of late-type stars during their main sequence (MS) phase has long been known to be correlated with rotation and anti-correlated with age (Skumanich 1972). This age-rotation-activity relation has been well-documented in the X-ray band which traces coronal and flare processes associated with the eruption of magnetic fields from the stellar interior onto the surface. Studies of young open clusters have documented a decay of average X-ray luminosities by two orders of magnitude from their arrival onto the Zero Age Main Sequence (ZAMS) to ages of several tenths of a Gyr (see reviews by Randich 1997; Jeffries 1999; Micela 2001; Favata & Micela 2003). The decay continues through the later 1 – 10 Gyr epochs (Güdel, Guinan, & Skinner 1997; Feigelson et al. 2004).

The commonly accepted explanation for this phenomenon is that late-type stellar magnetic activity is regulated principally by rotation (Pallavicini et al. 1981; Noyes et al. 1984; Baliunas et al. 1995), and its decay with stellar age is attributed to rotational braking due to mass loss. Ionized wind particles gain high specific angular momentum as they travel outward along spiral-shaped magnetic field lines that corotate with the star (Schatzman 1962; Kawaler 1988). Slower rotation presumably leads to reduced velocity shear at the tachocline between the radiative and convective zones, resulting in reduced magnetic field generation by the $\alpha - \Omega$ dynamo (Schrijver & Zwaan 2000).

X-ray studies of low-mass pre-main sequence (PMS) stars¹ have revealed very strong

¹X-ray emission is the most widely available tracer of surface magnetic activity for pre-main sequence and young main sequence stars (Feigelson & Montmerle 1999; Favata & Micela 2003). Chromospheric emission from optical and ultraviolet spectroscopic line indicators, such as H α or the Mg II lines, are often overwhelmed by emission attributed to accretion onto the surface. Nonthermal radio emission from flares can only occasionally be detected. In comparison, X-rays produced mainly by magnetic reconnection flares are seen in virtually all PMS stars across the Initial Mass Function and at all early phases of evolution from Class I protostars through the ZAMS (Getman et al. 2005b; Preibisch et al. 2005).

activity, exceeding the solar levels by several orders of magnitude both in time-averaged luminosity and power of individual flares (Feigelson & Montmerle 1999; Favata & Micela 2003; Güdel 2004). However, PMS activity does not exhibit the relationships to rotation and age seen along the MS. First, the rotational evolution is complicated by competition between an acceleration due to stellar contraction, a deceleration probably due to magnetic coupling between the outer layers and the circumstellar disk, and an uncertain coupling between inner and outer layers within the star (e.g. Bouvier, Forestini, & Allain 1997; Krishnamurthi et al. 1997; Barnes 2003a; Wolff, Strom, & Hillenbrand 2004). Second, the correlation between magnetic activity measured by X-ray luminosity and surface rotation is absent in PMS stars (Feigelson et al. 2003; Flaccomio et al. 2003a; Preibisch et al. 2005). This may either arise because the $\alpha - \Omega$ dynamo is saturated or, as these stars are often fully convective without a tachoclinical layer, because magnetic field generation is dominated by a turbulent convective dynamo that does not depend on rotation. Recent research thus establishes that the age-rotation and rotation-activity relations can not be readily extrapolated from the MS into the PMS regime.

We investigate here the third bivariate connection seen in MS stars: the age-activity relation. Past evidence for a decay in magnetic activity between $10^5 - 10^7$ yr before the star has begun to burn hydrogen has been unclear and ambiguous. Consider, for example, the stellar population of the Chamaeleon I cloud. From an *Einstein Observatory* study, Feigelson & Kriss (1989) reported an order of magnitude enhancement in the X-ray luminosity function (XLF) over that seen in the ZAMS Pleiades cluster. However, this was found to be wrong by the *ROSAT* study of the Chamaeleon I cloud which showed that *Einstein* sources were often poorly resolved blends of several closely spaced PMS stars and that the sample of weak-lined T Tauri stars was badly incomplete (Feigelson et al. 1993; Lawson, Feigelson & Huenemoerder 1996). The resulting XLF from this study showed little or no enhancement over ZAMS levels. Studies of portions of the extended Taurus-Auriga clouds indicated little decline in the X-ray luminosity function between the ages of PMS and Pleiades stars (Walter & Barry 1991; Briceno et al. 1997) although an enhancement in flare luminosities among PMS stars was noted (Stelzer et al. 2000). Kastner et al. (1997) compared average X-ray luminosities for a variety of young stellar clusters studied with *ROSAT* and found an increase of the median fractional X-ray luminosities by about one order of magnitude during the first 100 Myr, followed by a steep decay for older ages.

The contradictions among these early studies were likely due to combinations of several problems: different levels of incompleteness due to sensitivity limitations; incomplete cluster samples, particularly among X-ray faint weak-lined T Tauri stars; inadequate spatial coverage of nearby star formation regions subtending large regions of the sky; inadequate spatial resolution to resolve crowded regions; and inadequate hard energy sensitivity to penetrate

into embedded regions. The confounding influence of a strong statistical association between X-ray luminosity and mass (Preibisch et al. 2005) is particularly important: clusters studied with lower sensitivity tend to derive higher mean X-ray luminosities due to the failure to detect lower mass stars, leading to spuriously high levels of magnetic activity (Feigelson & Montmerle 1999; Preibisch & Zinnecker 2002; Feigelson et al. 2003).

These difficulties are largely overcome with the the *Chandra* Orion Ultradeep Project (COUP). It achieves high sensitivity $\log L_X \geq 27.0$ erg s⁻¹ with complete spatial coverage of the lightly obscured Orion Nebula Cluster (ONC) with spatial resolution ≥ 500 AU (Getman et al. 2005a). This gives a large unbiased sample of young stars down to the stellar limit; the L_X –Mass relation indicates it is >95%-complete X-ray detections above $\simeq 0.1 M_\odot$ (Preibisch et al. 2005). Furthermore, the sample is so large and well-characterized from optical study (Hillenbrand 1997) that the age-activity relation can be examined in mass-stratified subsamples. The Orion Nebula field also exhibits a range of ages within the PMS phase (Palla & Stahler 1999), allowing the study of X-ray evolution between $\sim 0.1 - 10$ Myr. COUP thus provides a unique opportunity to reexamine the PMS age-activity relationship in a reliable and quantitative fashion.

2. The COUP data

The COUP observation is the deepest and longest X-ray observation ever made of a young stellar cluster, providing a rich and unique dataset for a wide range of science studies. All observational details and a complete description of the data analysis can be found in Getman et al. (2005a). The total exposure time of the COUP image is 838 100 sec (232.8 hours or 9.7 days), and an source detection procedure located 1616 individual X-ray sources in the COUP image. The superb point spread function and the high accuracy of the aspect solution allowed a clear and unambiguous identification of most X-ray sources with optical or near-infrared counterparts with median offsets of $0.2''$. The remaining sources are a mixture of new PMS stars and unrelated extragalactic background sources (Getman et al. 2005b).

Spectral analysis was performed to produce an acceptable spectral model and to give reliable time-averaged broadband luminosities for as many as possible sources. A complete and detailed description of the spectral analysis can be found in Getman et al. (2005a), here we only summarize the main points. The XSPEC spectral fitting programme was used to fit the extracted spectra with one- or two-temperature optically thin thermal plasma MEKAL models (Mewe 1991), assuming 0.3 times solar abundances (Imanishi, Koyama, & Tsuboi 2001; Feigelson et al. 2002a) and X-ray absorption according to the atomic cross sections of Morrison & McCammon (1983) with traditional solar abundances to infer a total interstellar

column density.

We note that, in general, the resulting spectral parameters and their uncertainties are often not reliably determined, and alternative models may be similarly successful. In these cases, preference was given to the solution that avoids the inference of a very luminous, heavily absorbed, ultra-soft ($kT_1 < 0.5$ keV) component. The study presented in this paper, however, is not strongly affected by these uncertainties. The sample used for our analysis is restricted to optically visible T Tauri stars with modest extinction ($A_V \leq 5$ mag, corresponding to $\log N_H \lesssim 22$ cm⁻²), which are not affected by the greatest uncertainties in plasma temperatures and emission measures that occur for sources with high absorption, $\log N_H \simeq 22 - 23$ cm⁻².

The intrinsic, extinction-corrected, X-ray luminosities of the sources were computed by integrating the best-fit model source flux over the [0.5–8] keV band. The typical uncertainties in the derived X-ray luminosities of the stars in our sample are $\lesssim 30\%$. Note that these X-ray luminosities represent the average over the 10 days exposure time of the COUP dataset. This implies that the effect of short excursions in the X-ray lightcurves, like flares with typical timescales of a few hours, are “smoothed out”. The detection limit of the COUP data is $L_{X,\min} \sim 10^{27.0}$ erg/sec for lightly absorbed stars, and few sources appear near that limit.

We use the tabulated X-ray properties (and upper limits for the undetected ONC members) and identifications of the COUP sources listed in Tables 8, 9, and 11 in Getman et al. (2005a). Throughout this paper, we use the absorption-corrected X-ray luminosity in the 0.5 – 8 keV band, denoted $\log L_{t,c}$ by Getman et al. (2005a), for which we use here the simpler appellation, $\log L_X$.

3. Definition of the ONC low-mass star sample

The basis for the construction of the sample of well-characterized ONC stars used here is the study by Hillenbrand (1997) [H97 hereafter] of 1576 optically visible ($I < 17.5$) stars within ~ 2.5 pc ($\sim 20'$) of the Trapezium, for 934 of which optical spectral types are known. We used an updated version of the H97 tables in which spectral types and other stellar parameters for many objects have been revised (see Getman et al. 2005a). H97 discuss that, while their optical database is missing very low mass and heavily obscured objects, it is representative of all stars in the ONC region.

In this study, we use a homogenous, optically selected and extinction limited sample of low-mass ONC members. Our sample consists of those ONC stars from H97 which are: (i) located within the field-of-view of the COUP observation; (ii) not classified as unrelated

fore- or background stars on the basis of their proper motions; (iii) for which the optical extinction is known and is $A_V \leq 5$ mag; and (iv) for which masses and ages could be determined by comparison with the PMS models of Siess, Dufour, & Forestini (2000). A detailed discussion of these selection criteria is given in Preibisch et al. (2005). We further restrict our analysis to low-mass stars with $M \leq 2 M_\odot$. While the vast majority of these stars are clearly detected as X-ray sources in the COUP data, a few stars remained undetected. Most of the non-detections are due to X-ray source confusion in the COUP data; the typical case are close ($\sim 1'' - 2''$ separation) binary systems, in which only one of the components is clearly detected as an X-ray source (Getman et al. 2005b). In these cases, the object would perhaps have been detected if located at a different position. Since the occurrence of source confusion should not depend on stellar parameters, we consider these objects to be “unobserved” and ignore them in our analysis.

These criteria provide a sample of 481 ONC stars, 474 of which are detected as X-ray sources. With an X-ray detection fraction of 98.5%, we can be very confident that our conclusions will not be affected by non-detections. While our optical sample is not complete because spectral types are not available for all ONC stars, it should be a statistically representative sample of the ONC young stellar population with low extinction. The only potential systematic selection effect might be that some of the older ($\gtrsim 10$ Myr) very-low mass ($M \lesssim 0.2 M_\odot$) stars, such as reported by Slesnick et al. (2004), may be missing.

4. Evolution of X-ray activity within the age range of the ONC

4.1. ONC stellar age estimates

The large number of PMS stars with individual age estimates in our COUP sample provides an unique opportunity to look for possible relations between the X-ray activity and stellar age. The HR diagram for the ONC shows a wide spread of L_{bol} values at any given T_{eff} value, suggesting a considerable spread of stellar ages. The ages of the individual stars in our COUP optical sample derived from comparison of the HR diagram to the PMS models of Siess, Dufour, & Forestini (2000) range from $\log(\tau [\text{yr}]) = 2.7$ up to $\log(\tau [\text{yr}]) = 8.4$.

These values, however, have to be treated with caution. Inferred ages less than ~ 0.1 Myr are unreliable due to inadequate theoretical treatment of the stellar birth process. The extent of age spread between ~ 0.1 to ~ 10 Myr for the ONC stars has been debated (Hillenbrand 1997; Palla & Stahler 1999; Slesnick et al. 2004). Difficulties include choice of sample stars, choice of evolutionary tracks, and the empirical determination of the bolometric luminosities and effective temperatures. Bolometric luminosities have several potential sources

of errors including: intrinsic photometric variability, which can be very large for accreting systems; error in the estimation of the extinction, which is can be affected by circumstellar material; and the possible presence of unresolved binary companions, which causes systematic overestimation of the luminosity both because the two components light is attributed to the primary component and because the reddening is overestimated by a redder secondary. Unresolved binary companions can lead to overestimates of the luminosity by factors of two, what can lead to systematic underestimations of the true age up to factor of four. Errors in the determination of stellar effective temperatures affect the age estimates directly for the more massive ($M > 1 M_{\odot}$) stars, and indirectly (via errors in the amount of de-reddening and bolometric corrections) for the less massive $M < 1 M_{\odot}$ stars. We will therefore refer to the individual stellar age values derived from the observed HR-diagram as “isochronal ages” to make clear that they are not necessarily identical to the true stellar ages.

For the $M < 1 M_{\odot}$ stars we estimate that variability and extinction errors will typically cause an artificial spread in stellar luminosities of $\Delta \log L \sim \pm 0.1$, while the unresolved binary companions can cause a spread of $\Delta \log L \sim +0.3$. One might thus expect a perfectly coeval sample of stars to exhibit a scatter of $\Delta \log L \sim \binom{+0.4}{-0.1}$ around the isochrone in the observed HR diagram. The observed scatter in the HR diagram of the ONC is considerably larger than this with $\Delta \log L \sim 1.5$. We therefore concur with Palla & Stahler (1999) and Slesnick et al. (2004) that a true age spread of up to about a factor of 100 (from ~ 0.1 to ~ 10 Myr) is present in the ONC.

4.2. The dependence of X-ray emission on age within the ONC

With these caveats in mind, we can now look for the relations between X-ray activity and stellar (isochronal) age. As the evolutionary time scales for PMS stars are a strong function of the stellar mass (Preibisch et al. 2005), which itself has dependencies on bolometric luminosity, we believe it is necessary to consider mass stratified subsamples to avoid confusing interrelationships. We therefore consider four separate mass ranges: $0.1 - 0.2 M_{\odot}$, $0.2 - 0.4 M_{\odot}$, $0.4 - 1 M_{\odot}$, and $1 - 2 M_{\odot}$.

We also consider three measures of X-ray emission: the X-ray luminosity of the star, $\log L_X$ (in units of erg s^{-1}); the fraction of the bolometric luminosity emitted in the X-ray band, L_X/L_{bol} (in dimensionless units); and the X-ray surface flux, F_X (in units of $\text{erg}^{-1} \text{cm}^{-2}$). The fractional X-ray luminosity and X-ray surface flux are very similar to each other within a mass stratum, as they differ by T_{eff}^4 and PMS stars on the Hayashi convective tracks with similar masses also have similar surface temperatures. However, conceptually these are different indicators: the fractional luminosity tells the overall efficiency of the star in

converting luminous energy into magnetic activity, while the surface flux gives the average magnetic activity emissivity at the stellar surface.

The distribution function of these X-ray emission measures are not completely defined by the data because of the 7 undetected stars (all of which are in the two lower mass strata). To account for the non-detections, we construct the Kaplan-Meier maximum-likelihood estimator of the X-ray distribution functions. Similarly, for comparing two samples, seeking bivariate correlations and calculating linear regressions, we use statistical methods developed for ‘survival analysis’ which treat the non-detections in mathematically correct fashions (Feigelson & Nelson 1985). These calculations were performed with the *ASURV*² package. The probabilities that a correlation is present are calculated using a generalization of the nonparametric Kendall’s tau statistic. The linear regressions are calculated using the EM (Expectation-Maximization) Algorithm under the assumption of Gaussian residuals in the ordinate around the fitted line. The results of the statistical analysis are summarized in Table 1.

Figures 1–3 plot the X-ray indicators against isochronal stellar ages τ for our lightly absorbed optical sample. The X-ray luminosity (Figure 1) is seen to decrease with isochronal age from ~ 0.1 to ~ 10 Myr in all four mass ranges, though the effect is not strong. For the L_X vs. isochronal age diagram, the correlation tests in ASURV give probabilities ranging from 95% to 99.92% in the four mass strata that an anticorrelation is present. The slopes of the linear regression fits to the $\log(L_X) = a + b \times \log(\tau)$ relations with the EM algorithm range between $b \sim -0.2$ and $b \sim -0.5$ ³.

The fractional X-ray luminosity (Figure 2) shows an increase with isochronal age for the low-mass stars, but with lower statistical significance. The slopes of the linear regression fits to the $\log(L_X/L_{\text{bol}}) = a + b \times \log(\tau)$ relations with the EM algorithm are about $b \sim 0.3$ for the lower mass strata. The apparent decrease of L_X/L_{bol} with isochronal age in the $1 - 2 M_{\odot}$ mass range is not statistically significant.

²Astronomy SURVival analysis (LaValley et al. 1990) available from StatCodes <http://www.astro.psu.edu/statcodes>

³Since it is now well-established that X-ray luminosities of accreting PMS stars are systematically lower than non-accretion PMS stars (Flaccomio et al. 2003c; Preibisch et al. 2005), one might expect that L_X might increase with age rather than decrease as more accreting classical T Tauri stars evolve into non-accreting weak-lined T Tauri stars. We find that this effect does not dominate the stronger X-ray decay we find here. There are two reasons why this effect is minor: the population of accreting stars is relatively small compared to non-accreting stars in the ONC sample; and the difference in X-ray luminosities of the two classes is only $\Delta \log L_X \simeq 0.4$ which is relatively small compared to the full range of the XLFs.

The X-ray surface flux (Figure 3) also increases with isochronal age for the low-mass stars with correlation probabilities above 99% confidence for the low-mass ($< 1 M_{\odot}$) stars. The slopes of the linear regression fits to the $\log(F_X) = a + b \times \log(\tau)$ relations with the EM algorithm are $b \sim 0.3$. Again, no significant effect is found for the $1 - 2 M_{\odot}$ stars.

5. Long term evolution of X-ray activity

We now consider the temporal evolution of X-ray properties over a longer timescale by comparing the ONC PMS stars to samples of late-type stars in older star formation regions, the Pleiades, the Hyades and the solar neighborhood. We wish to trace the evolution of stars with fixed mass which, when comparing PMS and ZAMS stars, implies different spectral types. For example, according to the models of Siess, Dufour, & Forestini (2000), a $1 M_{\odot}$ star at the age of 1 Myr will have a spectral type of K5 rather than G2 on the main sequence. To match past treatments of this question, we consider here mass strata corresponding to the ZAMS spectral types: mass range $0.1 - 0.5 M_{\odot}$ corresponding to spectral types M0–M5; $0.5 - 0.9 M_{\odot}$ corresponding to K0–K9; and $0.9 - 1.2 M_{\odot}$ corresponding to G0–G9.

5.1. The comparison samples of stars

From Figures 1-3, we adopt an average age of 1 Myr for the ONC sample. We have selected for comparison two, somewhat older, PMS stellar clusters which have been well-studied with the *ROSAT* satellite: NGC 2264, with an adopted age of 1.7 Myr; and the Chamaeleon I star forming region with an adopted age 5.5 Myr (Flaccomio et al. 2003b). Due to sensitivity limitations, these samples are not available for the lowest mass stars.

To characterize young main sequence stars, we adopt the X-ray and optical data for the Pleiades and Hyades samples obtained from Stelzer & Neuhäuser (2001). These samples are based on *ROSAT* observations of optically selected members and therefore include upper limits for X-ray undetected stars. The Pleiades sample consists of 41 G-type stars (including 18 upper limits), 112 K-type stars (including 41 upper limits), and 62 M-type stars (including 27 upper limits). The Hyades sample consists of 22 G-type stars (including 2 upper limits), 51 K-type stars (including 6 upper limits), and 90 M-type stars (including 32 upper limits). We assume ages of 80 Myr for the Pleiades⁴ and 650 Myr for the Hyades.

⁴We note that recent age estimates for the Pleiades give a considerably higher age, perhaps 130 Myr. The uncertainty does not affect the conclusions drawn in this paper.

For older Galactic disk stars, we use the NEXXUS database (Schmitt & Liefke 2004) provides updated *ROSAT* X-ray and optical data (including accurate *HIPPARCOS* parallaxes) for a well-defined volume-limited samples of nearby field stars. The samples have 43 G-type stars (including 5 non-detections) within a limiting distance $d_{\text{lim}} = 14$ pc, 54 K-type stars (including 2 non-detections) within $d_{\text{lim}} = 12$ pc, and 79 M-type stars (including 5 non-detections) within $d_{\text{lim}} = 6$ pc. The NEXXUS tables were kindly provided to us by the authors; they list M_V , $B - V$, the X-ray luminosity L_X and the X-ray surface flux F_X . We calculate bolometric luminosities by interpolation from the main sequence relationship between M_V and L_{bol} . Although these stars possess a wide range of ill-determined ages, we adopt an average age of 3 Gyr for this sample.

5.2. Construction of the X-ray distribution functions

When comparing X-ray luminosities determined with different X-ray observatories, one has to take into account the different energy bands for which X-ray luminosities were computed. For Pleiades, Hyades, and nearby field stars considered here, the X-ray luminosities in the literature are given for the 0.1 – 2.4 keV *ROSAT* band. Conversion into the *Chandra* 0.5 – 8 keV band for comparison with our COUP results depends on the X-ray spectrum. We calculate the conversion factor using the PIMMS tool. For the moderately active ZAMS Hyads and Pleiads, we scale the *ROSAT* luminosities downward by 0.14 dex corresponding to a plasma temperatures $T = 10$ MK and consistent with the count-rate to luminosity transformation factor used by Stelzer & Neuhäuser (2001). For the NEXXUS stars, the count-rate to luminosity transformation factor used by Schmitt & Liefke (2004) is valid for a plasma temperature of $T \sim 2.5$ MK, and the corresponding *ROSAT* – *Chandra* band correction factor is -0.33 dex. The X-ray distribution functions, including the X-ray luminosity function (XLF), are the Kaplan-Meier estimators introduced in § 4.2.

5.3. Results

Figures 4–6 show the cumulative distribution functions of L_X , L_X/L_{bol} , and F_X for the ONC stars based on the COUP results in comparison with the older PMS samples, the ZAMS Pleiades and Hyades, and the solar neighborhood NEXXUS stars. The bottom right panels compare the median values of the X-ray activity in these samples as a function of stellar age.

The X-ray luminosities of Orion stars, in all of the mass strata, are highly elevated with

respect to all main sequence stars. For $\simeq 1 M_{\odot}$ stars, for example, the ONC sample is ~ 30 times stronger in X-ray luminosity than Pleiads or Hyads (Figure 4, top left). The fractional X-ray luminosities are elevated for stars $M > 0.5 M_{\odot}$ but not for lower mass (main sequence M-type) stars (Figure 5).

If we ignore the behavior within the PMS phase and consider only the longer-term decline from the ONC to the Pleiades, Hyades and nearby field star samples, a rough powerlaw decay in magnetic activity is seen for X-ray luminosities. For a relationship of the form $\log(L_X [\text{erg/sec}]) = a + b \times \log(\tau [\text{Myr}])$, we find slopes of $b = -0.76$ for the mass range $0.9 - 1.2 M_{\odot}$, $b = -0.78$ for $0.5 - 0.9 M_{\odot}$, and $b = -0.69$ for $0.1 - 0.5 M_{\odot}$. The decay in the other activity indicators, L_X/L_{bol} and F_X , is less rapid with $b \simeq -0.5$ for the higher-mass stars and $b \simeq -0.3$ for the $0.1 - 0.4 M_{\odot}$ stars. But the relationships here do not appear linear in the log-log diagrams of Figures 5-6. Rather the decay starts slowly and accelerates, though not as steeply as an exponential decay law as suggested by Walter & Barry (1991).

We also note that a global decay law for the whole age range ($10^6 - 10^{10}$ yr) may not imply a single physical mechanism here. Up to ages of a few 10 Myr, X-ray activity does *not* depend on the stellar rotation (Preibisch et al. 2005), the stellar interiors for most stars are fully convective, and the stars contract. On their approach to the main-sequence, the stars develop radiative cores, which probably enable $\alpha - \Omega$ type dynamo action. Finally, for the young main sequence stars a rotation-activity relation is well established (e.g. Pizzolato et al. 2003) and the subsequent decay in X-ray activity can be understood as the result of the wind-driven spin-down process. Therefore, it appears rather likely that the processes that determine the decline in X-ray activity at very young ages are different from those at ZAMS and later stages.

While the X-ray activity is clearly decreasing on long timescales, the evolution within the PMS epoch is less rapid. Our intra-ONC analysis (§ 4.2) shows a decay with powerlaw index $b \simeq -0.3$ ⁵. This decay is sufficiently slow that fractional X-ray luminosity and the X-ray surface flux is roughly constant or even *increases* over the age range $0.1 - 10$ Myr as the stars contract. Such a temporary increase in L_X/L_{bol} has been previously reported from an inter-cluster *ROSAT* study by Kastner et al. (1997).

⁵Comparison with the NGC 2264 and Chamaeleon I clusters suggests there may be no decay at all during the PMS phase (Figure 1), but there is some question whether these *ROSAT* surveys have sufficient resolution and sensitivity for reliable comparison with COUP. The intra-ONC analysis with uniformly excellent *Chandra* data suggest that the decay results in § 4.2 should be reliable.

6. Discussion

The COUP observation provides the most sensitive, uniform and complete study of X-ray properties for a PMS stellar population available to date. The extensive optical spectroscopy by Hillenbrand (1997), combined with evolutionary tracks of Siess, Dufour, & Forestini (2000), gives self-consistent ages for our sample with 481 stars of which 98.5% are detected in the COUP image. These ages range from ≤ 0.1 Myr to $\simeq 10$ Myr which covers a wide range of the PMS phases of low-mass stellar evolution. The large sample permits us to establish the evolution of X-ray luminosities (and the related activity indicators L_X/L_{bol} and F_X) with higher precision and reliability than possible from past studies. In particular, we examine activity evolution in mass strata to avoid the convolution of temporal and mass dependencies of magnetic activity that have confused previous studies. To establish the long-term evolution of magnetic activity, we compare our findings with mass-stratified XLFs obtained with the *ROSAT* satellite for older stars, particularly the Pleiades, Hyades, and a volume-limited sample of solar neighborhood stars.

Our fundamental result is that, treating the PMS phases as a whole, the X-ray luminosity decay law for stars in the $0.5 < M < 1.2 M_\odot$ mass range is approximately powerlaw with $L_X \propto \tau^{-0.75}$ over the wide range of ages $5 < \log \tau < 9.5$ yr. Studies of old disk stars suggest that this may steepen to $L_X \propto \tau^{-1.5}$ over $9.0 < \tau < 10.0$ yr (Güdel, Guinan, & Skinner 1997; Feigelson et al. 2004). We also note that Pace & Pasquini (2004) find evidence for a very steep decay of the chromospheric activity between $8.7 < \tau < 9.3$ yr. These results are similar to, but show more rapid decay than, the classical Skumanich (1972) $\tau^{-1/2}$ relation which had been measured for main sequence stars only over the limited age range $7.5 < \log \tau < 9.5$ yr. We also establish for the first time a mild decay in magnetic activity roughly as $L_X \propto \tau^{-1/3}$, for ages $0.1 < \tau < 10$ Myr within the PMS phase.

The magnetic decay is somewhat more complicated when other X-ray indicators and behavior within the PMS regime are considered. We find that the fractional X-ray luminosity L_X/L_{bol} and X-ray surface flux F_X exhibit an accelerating decay with age, falling slowly during the 1 – 100 Myr interval and faster on Gyr timescales on the main sequence.

While these results would appear to confirm and elaborate the long-standing rotation-age-activity relationship of solar-type stars, other recent *Chandra* studies (cf. § 1 and Preibisch et al. 2005) show that the rotation-activity relation is completely absent in PMS stars. We thus find the somewhat surprising result that the activity-age decay is strong across the entire history of solar-type stars but is not entirely attributable to rotational deceleration. A more complex astrophysical situation, perhaps involving both tachoclinical and convective dynamos as described by Barnes (2003a,b), is needed. Within the PMS phase when the star is still contracting, changes in the convective volume and surface area

may also be involved in the activity decay.

We furthermore show that the magnetic activity history for M stars with masses 0.1 to 0.4 M_{\odot} appears to be different. Only a mild decrease in X-ray luminosity, and even a mild increase in L_X/L_{bol} and F_X , is seen over the 1 – 100 Myr range, though the X-ray emission does decay over long Gyr on the main sequence. Although this result may be related to the well-established fact that the low-mass M stars have much longer rotational slow-down times than solar-type stars (e.g., Stauffer & Hartmann 1986), the non-existence of an activity-rotation relation for the $\sim 0.1 - 10$ Myr old ONC stars suggests that other astrophysical processes underlying the magnetic activity are responsible for this difference. Both PMS and main sequence dM stars are mostly or fully convective, and the unchanging fractional X-ray luminosity may represent the saturation of the magnetic dynamo processes in these convective stars. The difference in behavior compared to higher mass stars supports the idea that the dynamos in PMS and dM stars may be qualitatively different than in solar-type stars, arising from a dynamo powered by turbulence distributed throughout the convective interior rather than from rotational shear at the tachocline. These issues are further discussed in Mullan & MacDonald (2001), Feigelson et al. (2003), Barnes (2003b), and Preibisch et al. (2005).

While a comprehensive interpretation of our results in terms of dynamo theory is beyond the scope of this study, we believe they provide basic support for the idea that distributed convective dynamos are the dominant source of magnetic fields in PMS and dM stars.

COUP is supported by *Chandra* Guest Observer grant SAO GO3-4009A (E. Feigelson, PI). We would like to thank J.H.M.M. Schmitt and C. Liefke for information on the NEXXUS database, B. Stelzer and E. Flaccomio for X-ray data on young clusters, G. Micela and J.H. Kastner for thoughtful comments on the manuscript, and the referee, Manuel Guedel, for his detailed, insightful, and helpful comments on this paper.

Facility: CXO(ACIS)

REFERENCES

- Baliunas, S. L. et al. 1995, ApJ, 438, 269
 Barnes, S. A. 2003a, ApJ, 586, 464
 Barnes, S. A. 2003b, ApJ, 586, L145
 Audard, M., Güdel, M., Sres, A., Raassen, A. J. J., & Mewe, R. 2003, A&A, 398, 1137

- Bouvier, J., Forestini, M., & Allain, S. 1997, *A&A*, 326, 1023
- Briceno, C., Hartmann, L. W., Stauffer, J. R., Gagne, M., Stern, R. A., & Caillault, J. 1997, *AJ*, 113, 740
- Favata, F. & Micela, G. 2003, *Space Science Reviews*, 108, 577
- Feigelson, E. D. and Nelson, P. I. 1985, *ApJ*, 293, 192
- Feigelson, E. D. & Kriss, G. A. 1989, *ApJ*, 338, 262
- Feigelson, E. D., Casanova, S., Montmerle, T., & Guibert, J. 1993, *ApJ*, 416, 623
- Feigelson, E. D. & Montmerle, T. 1999, *ARA&A*, 37, 363
- Feigelson, E. D., Broos, P., Gaffney, J. A., Garmire, G., Hillenbrand, L. A., Pravdo, S. H., Townsley, L., & Tsuboi, Y. 2002a, *ApJ*, 574, 258
- Feigelson, E. D., Garmire, G. P., & Pravdo, S. H. 2002b, *ApJ*, 572, 335
- Feigelson, E. D., Gaffney, J. A., Garmire, G., Hillenbrand, L. A., & Townsley, L. 2003, *ApJ*, 584, 911
- Feigelson, E.D., Hornschemeier, A.E., Micela, G., Bauer, F.E., Alexander, D.M., Brandt, W.N., Favata, F., Sciortino, S., Garmire, G.P. 2004, *ApJ*, 611, 1107
- Flaccomio, E., Damiani, F., Micela, G., Sciortino, S., Harnden, F. R., Murray, S. S., & Wolk, S. J. 2003, *ApJ*, 582, 382
- Flaccomio, E., Damiani, F., Micela, G., Sciortino, S., Harnden, F. R., Murray, S. S., & Wolk, S. J. 2003b, *ApJ*, 582, 398
- Flaccomio, E., Micela, G., Sciortino, S. 2003b, *A&A*, 402, 277
- Getman, K. V., Flaccomio, E., et al., 2005a, *ApJS*, in press
- Getman, K. V., Feigelson, E. D., et al. 2005b, *ApJS*, in press
- Güdel, M. 2004, *A&A Rev.*, 12, 71
- Güdel, M., Guinan, E. F., & Skinner, S. L. 1997, *ApJ*, 483, 947
- Hillenbrand, L. A. 1997, *AJ*, 113, 1733
- Imanishi, K., Koyama, K., & Tsuboi, Y. 2001, *ApJ*, 557, 747

- Jeffries, R. D. 1999, ASP Conf. Ser. 158: Solar and Stellar Activity: Similarities and Differences, 75
- Kastner, J. H., Zuckerman, B., Weintraub, D. A., & Forveille, T. 1997, *Science*, 277, 67
- Kastner, J. H., Huenemoerder, D. P., Schulz, N. S., Canizares, C. R., & Weintraub, D. A. 2002, *ApJ*, 567, 434
- Kawaler, S. D. 1988, *ApJ*, 333, 236
- Krishnamurthi, A., Pinsonneault, M. H., Barnes, S., & Sofia, S. 1997, *ApJ*, 480, 303
- LaValley, M., Isobe, T. and Feigelson, E.D. 1990, *BAAS (Software Reports)*, 22, 917
- Lawson, W. A., Feigelson, E. D., & Huenemoerder, D. P. 1996, *MNRAS*, 280, 1071
- Mewe, R. 1991, *A&A Rev.*, 3, 127
- Micela, G. 2001, ASP Conf. Ser. 234: X-ray Astronomy 2000, 143
- Morrison, R. & McCammon, D. 1983, *ApJ*, 270, 119
- Mullan, D. J., & MacDonald, J. 2001, *ApJ*, 559, 353
- Noyes, R. W., Hartmann, L. W., Baliunas, S. L., Duncan, D. K., & Vaughan, A. H. 1984, *ApJ*, 279, 763
- Pace, G., & Pasquini, L. 2004, *A&A*, 426, 1021
- Palla, F. & Stahler, S. W. 1999, *ApJ*, 525, 772
- Pallavicini, R., Golub, L., Rosner, R., Vaiana, G. S., Ayres, T., & Linsky, J. L. 1981, *ApJ*, 248, 279
- Pizzolato, N., Maggio, A., Micela, G., Sciortino, S., & Ventura, P. 2003, *A&A*, 397, 147
- Preibisch, Th. & Zinnecker, H. 2003, *AJ*, 123, 1613
- Preibisch, Th., Kim, Y.-C., et al., *ApJS*, in press
- Randich, S. 1997, *Memorie della Societa Astronomica Italiana*, 68, 971
- Schatzman, E. 1962, *Annales d'Astrophysique*, 25, 18
- Schrijver, C. J. & Zwaan, C. 2000, *Solar and stellar magnetic activity*, New York:Cambridge University Press

- Schmitt, J.H.M.M., & Liefke, C. 1993, *A&A*, 417, 651
- Siess, L., Dufour, E., & Forestini, M. 2000, *A&A*, 358, 593
- Skumanich, A. 1972, *ApJ*, 171, 565
- Slesnick, C. L., Hillenbrand, L. A., & Carpenter, J. M. 2004, *ApJ*, 610, 1045
- Soderblom, D.R., Stauffer, J.R., Hudon, J.D., Jones, B.F. 1993, *ApJS*, 85, 315
- Stauffer, J.R., & Hartmann L.W. 1986, *PASP*, 98, 1223
- Stelzer, B., Neuhäuser, R., & Hambaryan, V. 2000, *A&A*, 356, 949
- Stelzer, B., & Neuhäuser, R. 2001, *A&A*, 377, 538
- Walter, F. M. & Barry, D. C. 1991, in *The Sun in Time* (C. P. Sonnett, ed.), Univ. Arizona Press, 633
- Wolff, S. C., Strom, S. E., & Hillenbrand, L. A. 2004, *ApJ*, 601, 979

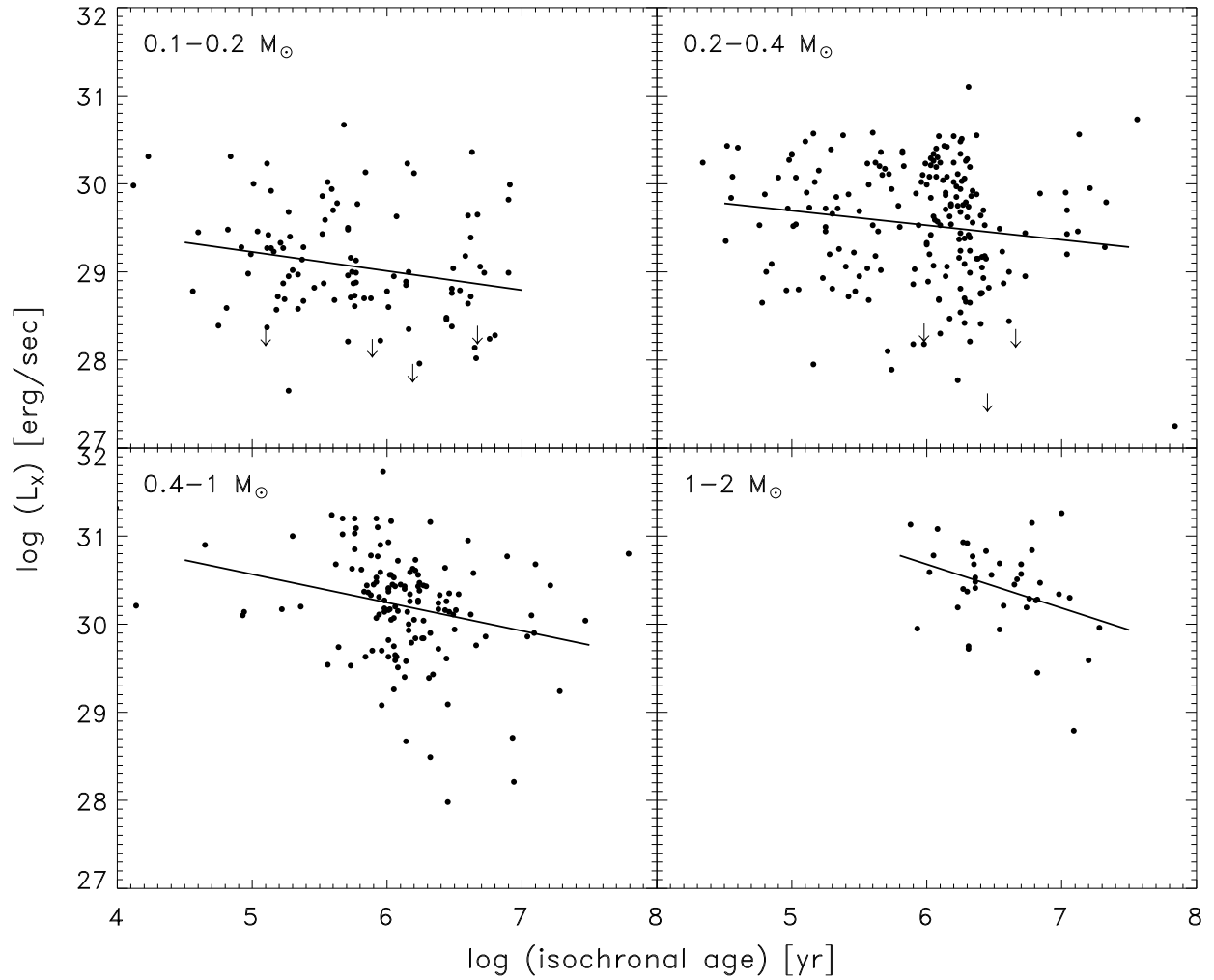


Fig. 1.— X-ray luminosity versus stellar age for the stars in the COUP ONC sample separated in four mass ranges. The lines shows the linear regression fits computed with the EM Algorithm.

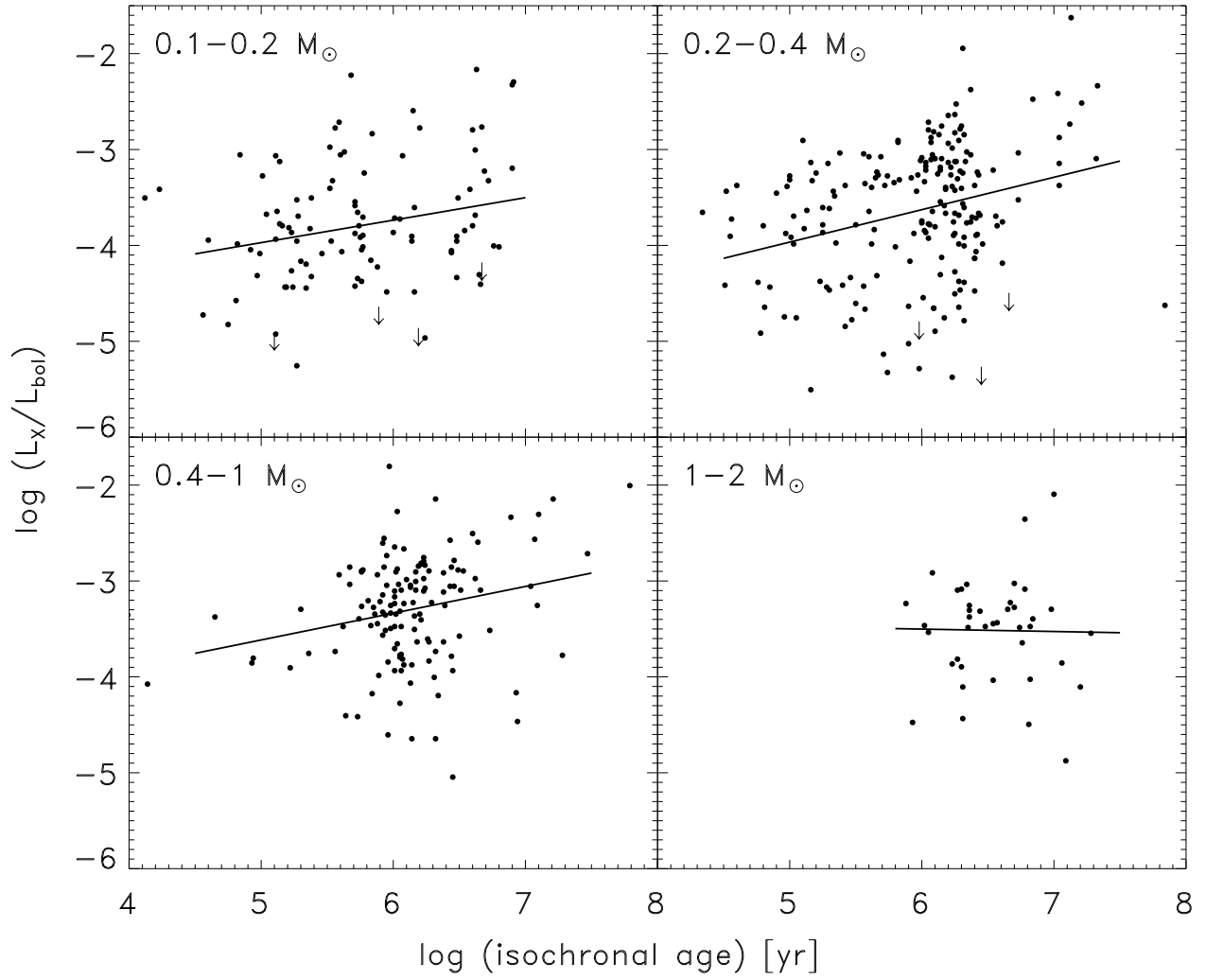


Fig. 2.— Fractional X-ray luminosity versus stellar age. Stellar sample and fits are as described in Figure 1.

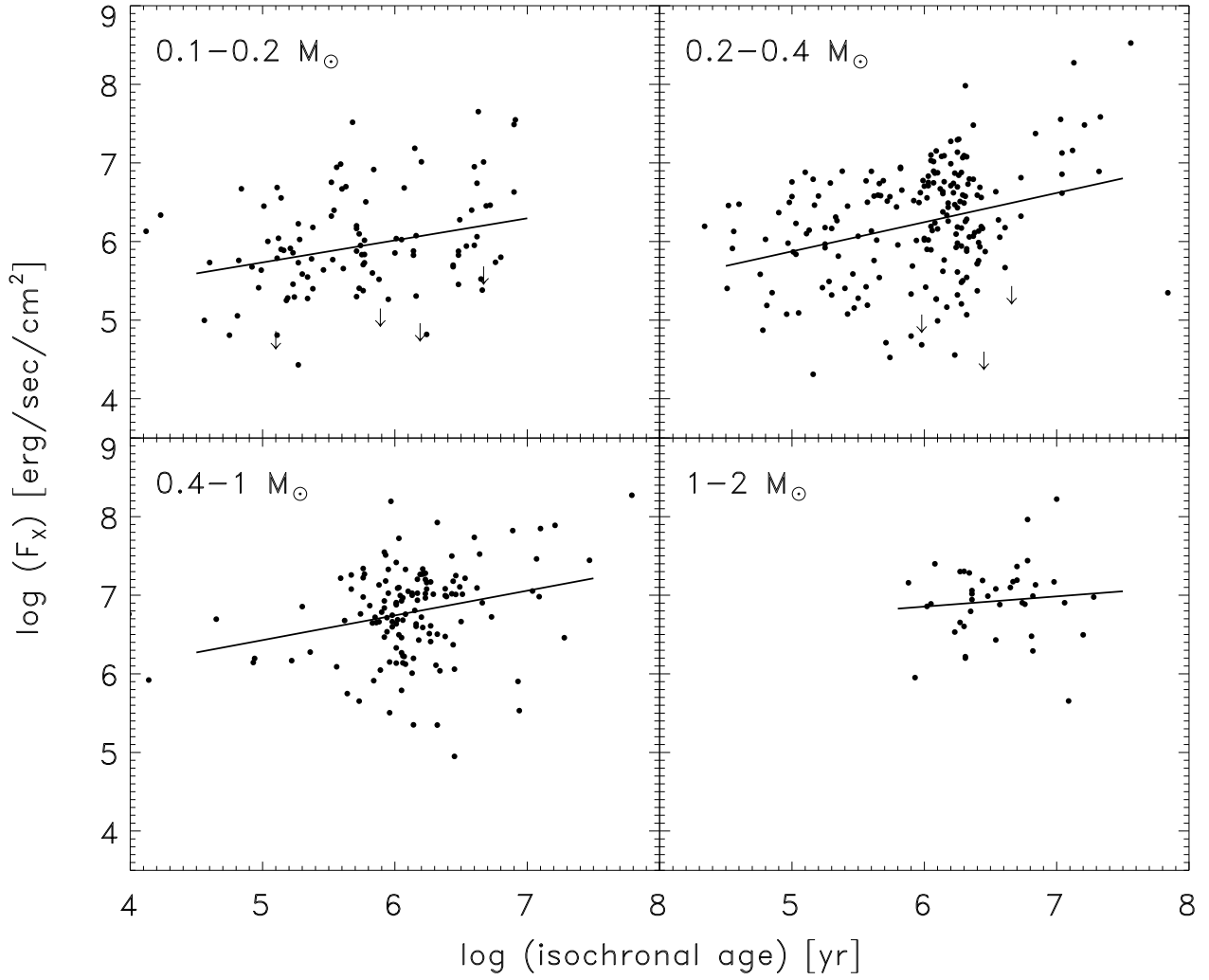


Fig. 3.— X-ray surface flux versus stellar age. Stellar sample and fits are as described in Figure 1.

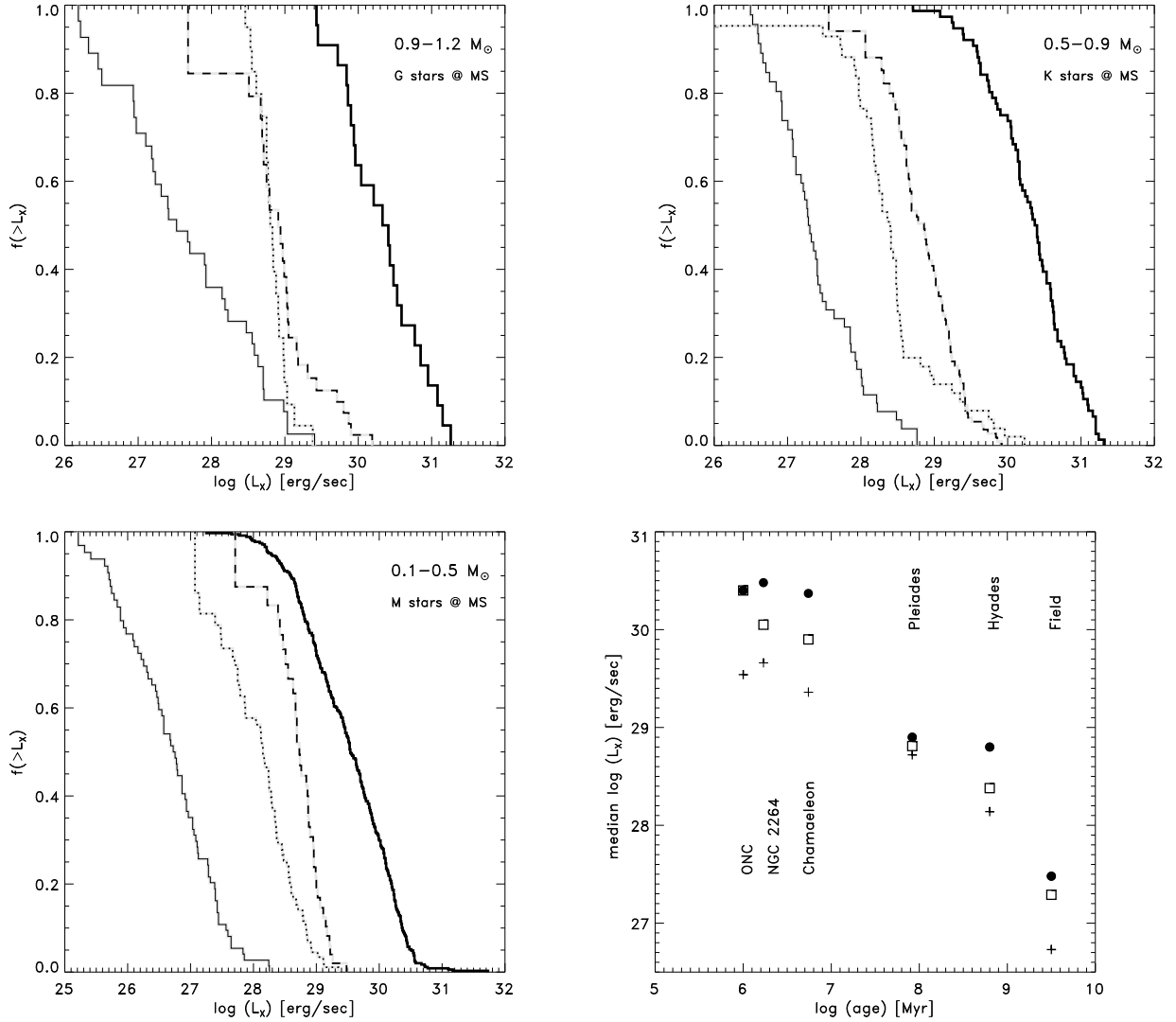


Fig. 4.— Evolution of the X-ray luminosity from the pre-main sequence through the main sequence. The first three plots show the cumulative X-ray luminosity functions (XLFs) for three mass ranges. In each panel, the thick solid line shows the COUP X-ray luminosities for our ONC sample, the dashed line shows the Pleiades, the dotted line the Hyades, and the thin solid line the field stars from NEXXUS. The lower right panel shows the median X-ray luminosity in each sample and mass range as a function of the age. The solid dots show the 0.9–1.2 M_{\odot} (G-type on the main sequence) stars, squares show the 0.5–0.9 M_{\odot} (K-type on the main sequence) stars, and crosses the 0.1–0.5 M_{\odot} (M-type on the main sequence) stars.

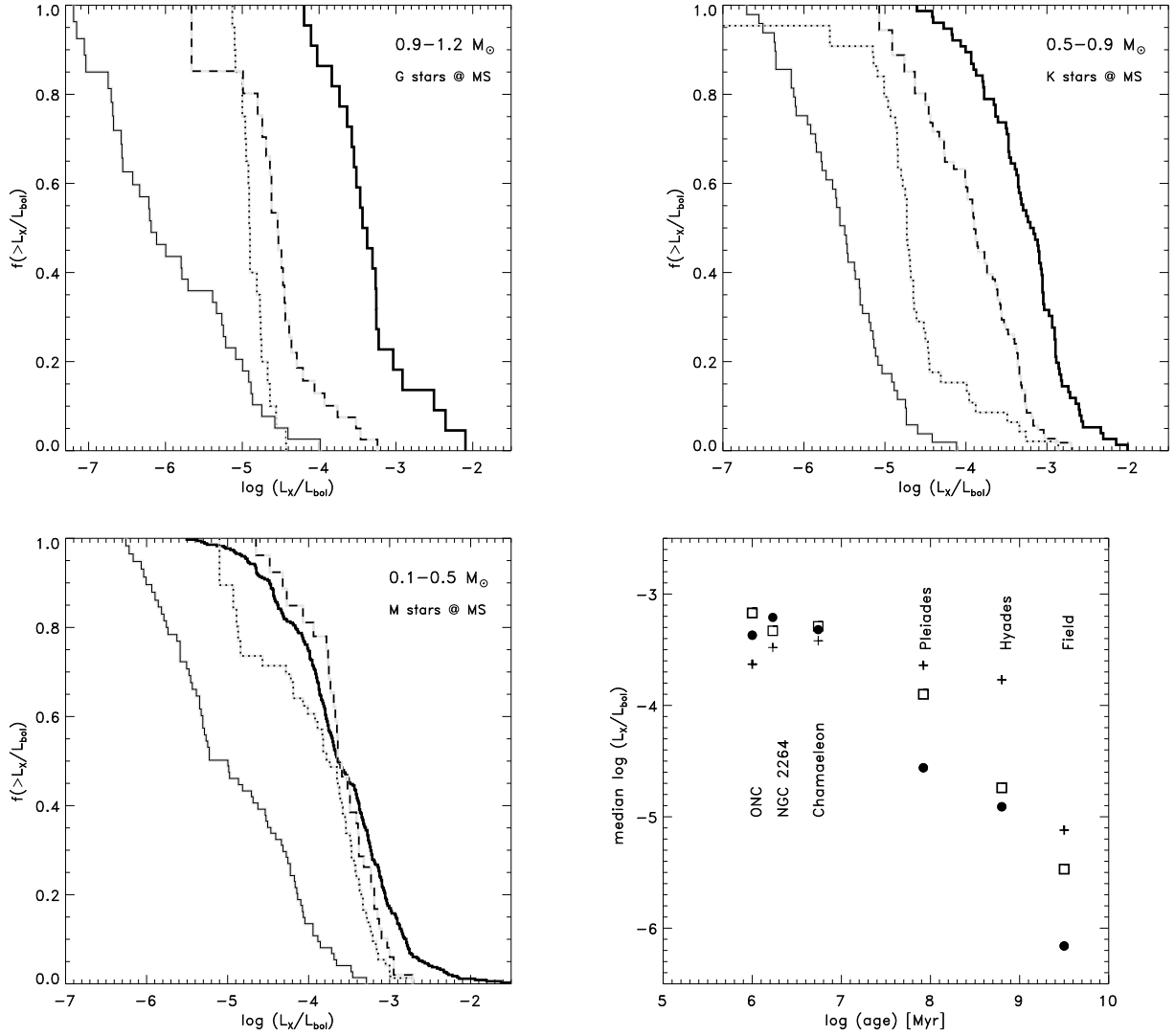


Fig. 5.— Evolution of the fractional X-ray luminosity. The lines and symbols are defined in the Figure 4 caption.

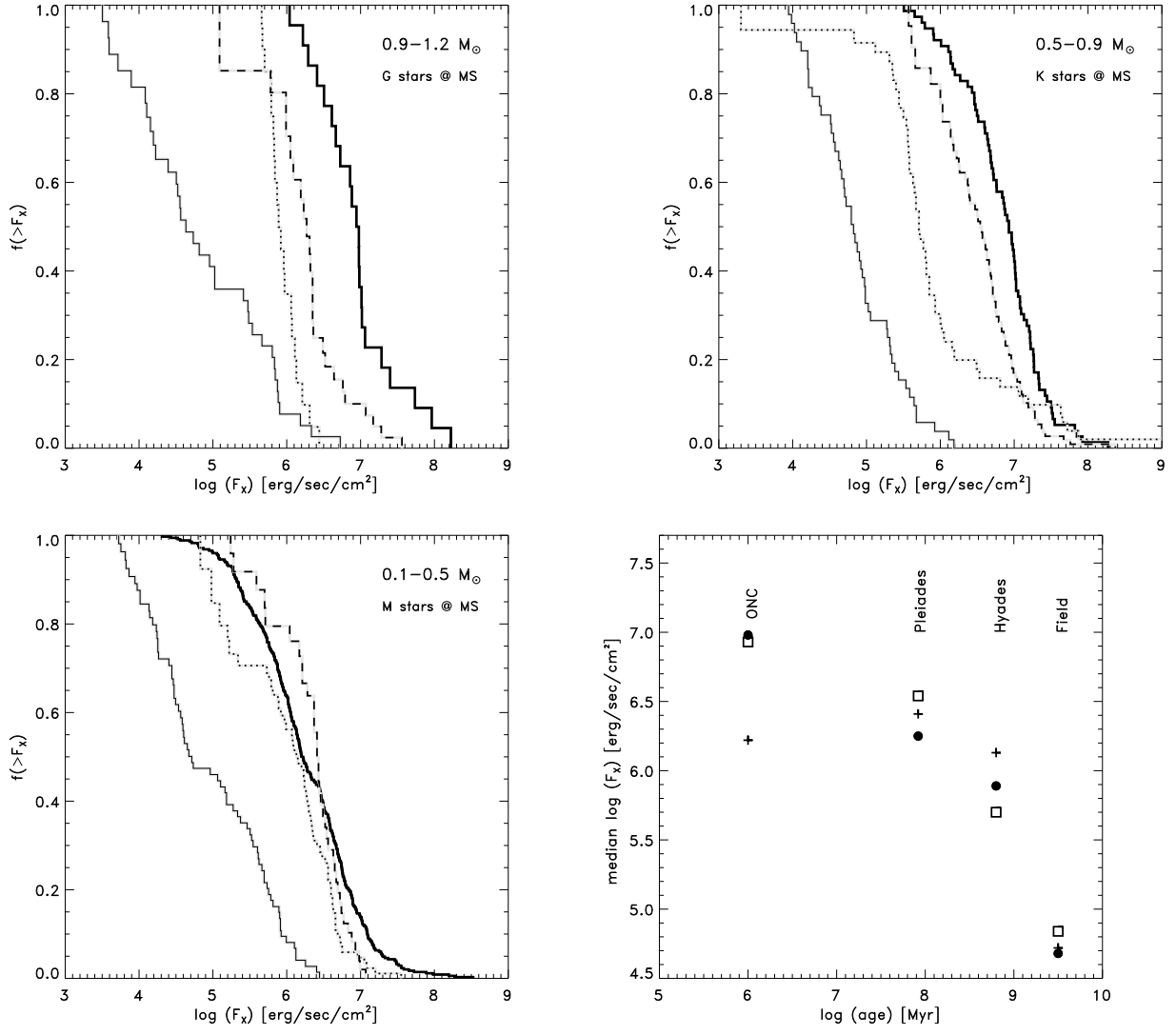


Fig. 6.— Evolution of the X-ray surface flux. The lines and symbols are defined in the Figure 4 caption.

Table 1. X-ray activity versus isochronal age correlations for the ONC stars

Mass range [M_{\odot}]	$P(0)$	a	b
(a) $X = L_X$			
0.1 – 0.2	0.021	30.31 ± 0.57	-0.22 ± 0.09
0.2 – 0.4	0.018	30.52 ± 0.48	-0.17 ± 0.08
0.4 – 1.0	0.001	32.17 ± 0.60	-0.32 ± 0.10
1.0 – 2.0	0.053	33.66 ± 1.39	-0.50 ± 0.21
(b) $X = L_X/L_{\text{bol}}$			
0.1 – 0.2	0.030	-5.14 ± 0.53	0.23 ± 0.09
0.2 – 0.4	0.001	-5.66 ± 0.48	0.34 ± 0.08
0.4 – 1.0	0.010	-5.01 ± 0.57	0.28 ± 0.09
1.0 – 2.0	0.789	-3.35 ± 1.62	-0.02 ± 0.25
(c) $X = F_X$			
0.1 – 0.2	0.008	4.33 ± 0.53	0.28 ± 0.09
0.2 – 0.4	0.001	4.02 ± 0.48	0.37 ± 0.08
0.4 – 1.0	0.008	4.86 ± 0.57	0.31 ± 0.09
1.0 – 2.0	0.499	6.08 ± 1.45	0.13 ± 0.22

Note. — This table summarizes the results of the correlation analysis for the relations between X-ray activity and isochronal age of the form $\log(X) = a + b \times \log(\tau)$. We list the probabilities $P(0)$ that no correlation is present found with the generalized nonparametric Kendall’s tau statistic and the coefficients of the linear regressions calculated using the EM Algorithm in ASURV.